

## Targeting Annexin A2 gene for Suppressing Invasion and Tumor Progression of Liver Cancer

Yao Min, Wang Li, Yan Meijuan, Gu Xing, Yan Xiaodi,  
Zhang Haijian and Dengfu Yao\*

Research Center of Clinical Medicine, Affiliated Hospital of  
Nantong University, Nantong, Jiangsu, China.

(Received: 03 March 2013; accepted: 14 April 2013)

Up-regulation of Annexin A2 (ANXA2) expression is associated with the tumorigenesis and development, but the effect of small hairpin RNA (shRNA) targeting ANXA2 on cell invasion and tumour progression in hepatocellular carcinoma hasn't been reported up to now. In this study, the expression level of ANXA2 in MHCC97-H cells with high metastasis potential was the highest among that in 4 hepatoma cell lines and about 9 times as high as that of hepatocyte LO2 cells. The shRNA targeting ANXA2 specially and effectively inhibited its expression at both protein and mRNA level. ANXA2 was mainly localized in cell membrane and cytoplasm, feebly in cell nucleus. Moreover, ANXA2 silencing obviously suppressed the cell proliferation in vitro ( $P < 0.05$ ), while the inhibiting rate of tumor growth was 38.24% in vivo. The S phase percentage of MHCC97-H/shRNA cells was dramatically decreased from 36.14% down to 27.76%. Furthermore, ANXA2 silencing inhibited the invasion and migration potential of MHCC97-H cells, and the percentage of invading cells decreased from 86.14% down to 52.16%, while the relative migration distance of MHCC97-H/shRNA group decreased down to 60.53%. Taken together, these data demonstrated that the shRNA targeting ANXA2 inhibited high metastasis potential hepatoma cell invasion, migration and tumor progression, which provided further insight into understanding the pathogenesis of HCC and seeking for appropriate treatment.

**Key words:** Annexin A2, Small hairpin RNA, HCC, Invasion, migration, Tumor progression.

Hepatocellular carcinoma (HCC<sup>1</sup>), as the 3<sup>rd</sup> leading cause of cancer-related death, is increasing in worldwide incidence and is strongly associated with chronic liver disease and cirrhosis (Forner, *et al.*, 2012). Surgical therapy with liver transplantation or resection remains the mainstay of curative therapy for patients in the early stage of HCC (DuBray, *et al.*, 2011). However, even with radical resection, 60~70% of patients develop metastasis and recurrence within 5 years of surgery (Marquardt, *et al.*, 2012). Thus, it is urgent to study

the pathogenesis of HCC. Recent studies show that Annexin A2 (ANXA2) plays an important role in malignant transformation and development of HCC (Lokman, *et al.*, 2011;). ANXA2 is a calcium-dependent phospholipid-binding protein (Flood and Hajjar, 2011).

ANXA2 expression and its phosphorylation at residues of tyrosine 23 by c-Src are up-regulated in HCC, while tyrosine 23 phosphorylation-dependent cell-surface localization of ANXA2 is required for invasion and metastases of pancreatic cancer (Zheng, *et al.*, 2011). Moreover, accumulating evidence indicates that ANXA2 promotes tumor metastasis by inducing the conversion of plasminogen to plasmin, which leads to activation of metalloproteinases and degradation of extracellular

\* To whom all correspondence should be addressed.  
Tel: +86-513-85052297;  
E-mail: yaodf@ahnmc.com

matrix components (Sharma M., *et al.*, 2010). However, the effect of small hairpin RNA (shRNA) targeting ANXA2 on cell invasion and tumor progression in hepatocellular carcinoma hasn't been reported up to now. In this present study, the expression and distribution of ANXA2 were investigated in different HCC cell lines and focused on exploring the effects of shRNA targeting ANXA2 on cell invasion and tumor progression in hepatocellular carcinoma.

## METHODS

### Plasmid construction

ANXA2-specific shRNA corresponding to nucleotides 94~113 downstream of the transcription start site of ANXA2 was synthesized as described (Ohno, *et al.*, 2009), and inserted into BamHI-HindIII linearized pRNAT-U6.1/NeoshRNA expression vector in Biomics Biotechnologies Co., Ltd., China. The negative control vector contains a shRNA insert that does not suppress the expression of genes expressed in humans, rats, or mice. All inserted sequences were verified by DNA sequencing. The plasmids were named as pRNAT-U6.1-shRNA and pRNAT-U6.1-negative, respectively.

### Cell culture and transfection

HepG2, SMMC-7721, SMMC-7402, and LO<sub>2</sub> cell lines were obtained from Biomics Biotechnologies Co., Ltd. China. All the cells were grown in DMEM (Life Technologies, USA) with 10 % FBS at 37°C in a humidified atmosphere of 5 % CO<sub>2</sub>. Until growing to 90%~95% confluency, the MHCC97-H cells were transfected with the pRNAT-U6.1-shRNA and pRNAT-U6.1-negative plasmids using ployJet™ in vitro DNA transfection reagent (SignaGen, USA) according to the manufacturer's instructions. After transfected for 48 h, screening test was carried out with a medium containing 400 µg/mL of G418 (Life Technologies, USA) for 14 days and later always with 200 µg/mL of G418, and then the cell lines were named as the MHCC97-H/shRNA and MHCC97 -H/negative group, respectively. MHCC97-H cells without transfection were named as the MHCC97 -H/mock group.

### RNA isolation and cDNA synthesis

Total RNA was isolated from 50 mg of liver tissue, using Trizol reagent (Life Technologies, Inc., USA) according to the manufacturer's

instructions. The integrity of the total RNA was examined by 1 % agarose gel electrophoresis, the quantity was determined based on absorbance at A<sub>260</sub>, and the purity was analyzed based on the absorbance ratio at A<sub>260/280</sub> (Bio-RAD smartspec™ plus, Bio-Rad Life Science Res. and Dev. Co., Ltd., China). The cDNA was synthesized from 1 µg of total RNA using 1st strand cDNA synthesis kit (Fermentas Inc., Canada) according to the manufacturer's instructions.

### Quantitative PCR (qPCR)

The qPCR was run on an Applied Biosystems stepone™ real time PCR system according to the manufacturer's recommendations (Life Technologies, Inc., USA). The solution contained 25µL 2×SYBR Premix Ex Taq (Takara Co., Ltd., China), 2 µL primer mix, 1µL 50×ROX Reference Dye I, 4µL cDNA, and 18µL deionized water to make a total volume of 50 µL. The primers were as follows: ANXA2 forward, 5'-TGA GCGGATGCTTTGAAC-3', ANXA2 reverse, 5'-ATC CTGTCTCTGTGCATTGCTG-3'.  $\beta$ -actin used as an internal control with a set of primers, forward, 5'-ATT GCCGACAGGATGCAGA-3', and reverse, 5'-GAGT ACTTGCGCTCAGGAGG A-3', as described (Ohno, *et al.*, 2009).  $\beta$ -actin was run in each reaction while no template (H<sub>2</sub>O) control was included in each run. The optimized PCR conditions were as follows: 1 cycle at 95 °C for 2 min; 40 cycles of 95 °C for 10 sec, 62 °C for 1 min and final extension at 60 °C for 15 sec. The relative quantitative analysis was performed by comparison of the 2<sup>-Ct</sup> values.

### Western blotting

Cell protein extracts were collected and determined using an enhanced BCA assay kit (Beyotime, China). 20 mg of protein from each sample was run on a 15 % SDS-PAGE, then transferred onto PVDF membranes, blocked in 5 % BSA in Tris-buffered saline, immunoblotted overnight at 4°C with the anti-ANXA2 and anti- $\beta$ -actin antibodies (Santa Cruz, USA) followed by respective horseradish peroxidase-conjugated secondary antibodies. The bands were subsequently visualized by a chemiluminescence detection system (Milipore Corp., USA) with an image analyzer. ANXA2 was expressed with relative ratio, calculated by the formula using signal ANXA2 intensity and  $\beta$ -actin. RR=SIANXA2/SI  $\beta$ -actin.

**Immunofluorescence assay**

Cells were cultured for 24 h on cover slips in 24 well plates and washed thrice with PBS, fixed with 4 % paraformaldehyde for 10 min, and then blocked in PBS containing 3 % BSA for 30 min at 37 °C. The samples were incubated in the monoclonal primary antibody rabbit anti-human ANXA2 (1:100 dilution) overnight at 4°C. After washed thrice with PBS, cells were incubated with Cy3-labeled goat anti-rabbit IgG secondary antibody (1:500 dilution) for 1 h at 37°C in dark, washed thrice with PBS for 5 min, stained with 4', 6-diamidino-2-phenylindole for 5 min and washed thrice, and finally sealed with 50 % glycerin. Observations were performed under multifunction microscope (Olympus IX71, Japan).

**Cell proliferation assay**

Cell proliferation was evaluated using a cell counting kit-8 (CCK-8, Beyotime Institute of Biotechnology, Haimen, China) according to the manufacturer's instructions. MHCC97-H/mock, MHCC97-H/shRNA, MHCC97-H/negative, and LO2 cells were seeded in 96-well plates (2×10<sup>3</sup> cells/well with 100 µL medium, each group of 5 wells) and cultured for 24h. 10 µL of CCK-8 solution was added to the culture medium for 2 h, and then A450 was recorded by a microplate reader (BioTek, USA), which was repeated at different time points. Experiments were performed in triplicate and repeated 5 times.

**Cell cycle assay**

Cell cycle assay was performed using cell cycles, and apoptosis analysis kit according to the manufacturer's instructions. MHCC97-H/mock, shRNA, negative, and LO2 cells were seeded at 1.0×10<sup>6</sup> cells/well (6 well plate) and cultured for 24h. Subsequently, the cells were digested with trypsin enzyme, washed with PBS, and fixed for 24h at 4°C in 70% ethanol. The cells were stained with propidium iodide, and analyzed by flow cytometry to investigate cell cycle (BD FacsCalibur, China). Experiments were performed in triplicate and repeated thrice (Gao, *et al.*, 2011).

**Transwell assay**

The MHCC97-H/mock, MHCC97-H/shRNA, MHCC97-H/negative, and LO2 cells were plated at 1.0×10<sup>5</sup> cells/well in 0.5 mL of serum-free medium in 24-well matrigel-coated transwell units with polycarbonate filters (Costar Inc., Milpitas, USA) containing 8-µm pores. The outer chambers

were filled with 0.5 mL of medium containing 10 % FBS. After 24 h, the cells were fixed in methanol and stained with crystal violet. The top surface of the membrane was gently scrubbed with a cotton bud, and the cells invading through the membrane filters were counted on glass slides, and images were captured using an inverted microscope equipped with a CCD camera (Olympus IX71, Olympus Corp., Tokyo, Japan).

**In vitro wound-healing assay**

HCC cells were cultured in 12-well plates until sub-confluent. Scratches were introduced to the cell monolayer, using a plastic pipette tip. The cells were washed with serum-free medium and cultured in RPMI 1640 medium with 0.1 % FBS. Photo-micrographs at 10× objective magnification were taken at various time points (0 h and 24 h). Relative migration distance was calculated by following formula: the distance (%) = 100 (AX – BX)/(A<sub>mock</sub> – B<sub>mock</sub>), where A is the width of the cell wounds before incubation and B is the width of the cell wounds after incubation (Zhao, *et al.*, 2011).

**Xenograft tumor-growth assay**

Sixteen BALB/C nude mice at age of 6 week old (SPF degree), body weight 20±3g from the Shanghai Super-B&K laboratory animal Co., Ltd., China were randomly divided into 4 groups: MHCC97-H/mock-, negative-, shRNA-, and control group (4 mice/group). Cells (2×10<sup>7</sup>/mouse) suspended in 0.2 ml DMEM were injected subcutaneously into the nude mice at the right flank. Tumor size was measured using calipers at the indicated time points. Tumor volume was calculated according to the formula: volume = length × width<sup>2</sup>/2. The animals were sacrificed on the 21<sup>st</sup> day after injection. Tumor was dissected and weighed. The tumorigenicity inhibition rate was calculated as ((tumor weight<sub>control</sub> - tumor weight<sub>shRNA</sub>)/ tumor weight<sub>control</sub>) × 100 % (Ruan, *et al.*, 2011).

**Pathological examination**

The Hematoxylin and Eosin staining (H&E Staining) was performed according to the manufacturer's instructions (Beyotime Institute of Biotechnology, Haimen, China). Dehydrated 3 µm thick tissue sections were immersed for 2 min in distilled water, stained with haematoxylin for 5 min, washed thrice with tap water for 5 min, dehydrated with 95 % ethanol for 5 sec, stained with eosin for

2 min, washed twice with 70 % ethanol for 5 min, and then dehydrated, air dried, and mounted.

### Immunohistochemistry

Immunohistochemical analysis was performed using immunostain elivision kit according to the manufacturer's instructions (Maxim Biotech Inc., California, USA). In detail, the percentage of positive cells was assessed semiquantitatively and classified as follows (Wang D., *et al.*, 2011).

### Statistical analysis

Results are expressed as mean  $\pm$  SD. The bands by Western blotting were relatively analyzed with the Image J analysis software (Version 1.30v). Analysis was carried out by one-way analysis of variance followed by the least difference test or Newman-Keuls test.  $P < 0.05$  was considered significant.

## RESULTS AND DISCUSSION

### ANXA2 expression of different HCC cells

No effective therapeutic option exists for the treatment of the major HCC patients (El-Serag, 2011). Analysis of ANXA2 gene transcription in HCC cells are shown in Table 1. ANXA2 expression in different cells is shown in Figure 1. ANXA2 was up-regulated in 4 kinds of hepatoma cells and was the highest level in MHCC97-H cells with high metastasis potential, whether at protein or mRNA level, suggesting that over-expression of ANXA2 may be associated with high metastasis potential and invasion ability of HCC cells.

### Inhibition of ANXA2 expression by shRNA in MHCC97-H cells

The alteration of ANXA2 expression at mRNA level after the cells transfected with specific shRNA is shown in Table 2. ANXA2 mRNA in the shRNA group stably expressing shRNA was significantly lower ( $P < 0.01$ ) than that in the negative or the mock group. ANXA2 expression at protein and the ratio of ANXA2 relative to  $\beta$ -actin after the cells transfected with shRNA demonstrated that ANXA2 expression in the shRNA group was decreasing significantly, and but not in the negative group or the mock group.

### Distribution of ANXA2 Expression after shRNA Transfection

ANXA2 expression in the MHCC97-H / shRNA group reflecting the silence efficiency from

the perspective of morphology is shown in Figure 2. The nucleus of MHCC97-H/mock cells, marked with DAPI dye, showed some fragmented nuclei with condensed chromatin comparing with the cells in the MHCC97-H/mock group or the MHCC97-H/negative group. Targeting ANXA2 inhibited the expression of ANXA2 and mRNA with the efficiency up to above 80%.

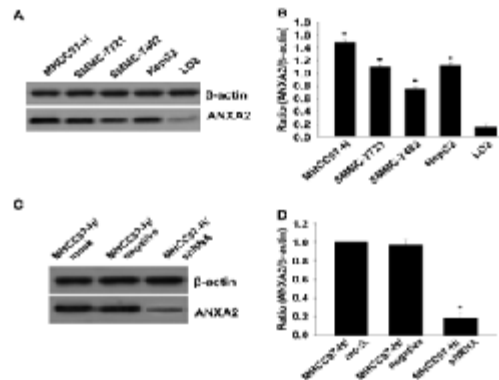


**Fig. 1.** ANXA2 expression in hepatoma cells or MHCC97-H cells transfected with ANXA2 shRNA

(A) Western blotting ( $n=3$ , mean  $\pm$  SD). (B) ANXA2 expression in MHCC97-H cells was the highest among 4 cell lines, and 8 times higher than that in LO<sub>2</sub> cell lines ( $*P < 0.01$ ). (C) The ratio of ANXA2 to  $\beta$ -actin. (D) ANXA2 level in MHCC97-H cells with shRNA was effectively inhibited ( $*P < 0.01$ ), but there was no statistical difference between the mock group and the negative group.

### shRNA inhibited growth of MHCC97-H cells

The effect of ANXA2 shRNA on proliferation and cell cycles of MHCC97-H cells transfected with specific shRNA is shown in Figure 3. The effect of shRNA targeting ANXA2 on cell cycles is shown in Table 3. Moreover, ANXA2 silencing down-regulates the levels of S100A10, c-Myc, and plasmin and inhibits breast cancer cell proliferation (Zhang, *et al.*, 2010).

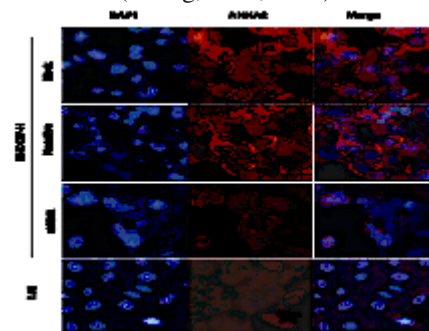
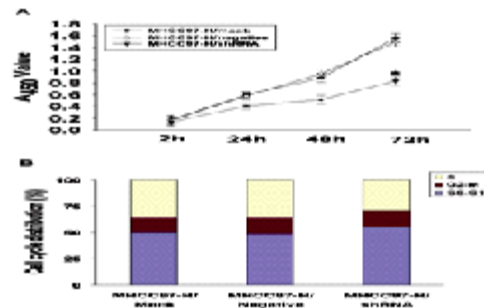


**Fig. 2** Expression and distribution of ANXA2 after MHCC97-H cells transfected with specific shRNA

Representative photos (400×mag.). ANXA2 was mainly localized in membrane and cytoplasm, feebly in nucleus. MHCC97-H/shRNA cells showed obviously weaker red signal in membrane or cytoplasm comparing with the MHCC97-H/mock cells or the negative cells.

### Silencing ANXA2 suppressed invasion of MHCC97-H cells

The effect of ANXA2 silencing on the invasion and migration potential of MHCC97-H cells transfected with specific shRNA in vitro is shown in Figure 4. These results suggested that the invasion and migration potential of HCC cells is correlated with ANXA2 expression level, and ANXA2 silencing is sufficient to inhibit invasion



(A) Cellular proliferation assay with CCK8. (B) Cell cycle assay with propidium iodide staining. Cells were stained with propidium iodide and cell cycle distribution was analyzed by flowcytometry as shown (n=3).

**Fig. 3** Effect of ANXA2 suppression on proliferation and cell cycles of MHCC97-H cells

**Table 1.** Analysis of ANXA2 mRNA expression in 4 kinds of HCC cells with LO2 cells.

Group	n	Ct <sub>ANXA2</sub>	Ct <sub>β-actin</sub>	2 <sup>-ΔΔCt</sup>	q	P value
LO2	5	25.16 ± 0.09	20.86 ± 0.03	1.00		
HepG2	5	22.14 ± 0.15	20.66 ± 0.02	7.07 ± 0.35	32.200*	< 0.001
SMMC-7402	5	22.87 ± 0.15	20.80 ± 0.14	4.68 ± 0.31	19.517*	< 0.001
SMMC-7721	5	22.21 ± 0.12	20.72 ± 0.10	7.02 ± 0.19	31.923*	< 0.001
MHCC97-H	5	21.85 ± 0.26	20.78 ± 0.13	9.45 ± 0.53	44.814*	< 0.001

\*Compared with the LO<sub>2</sub> group. n, number of independent sample.

**Table 2.** Specific shRNA down-regulated ANXA2 mRNA expression of MHCC97-H cells

Group	n	Ct <sub>ANXA2</sub>	Ct <sub>β-actin</sub>	2 <sup>-ΔΔCt</sup>	q	P value
MHCC97-H/mock	5	21.84 ± 0.11	20.77 ± 0.16	1.00		
MHCC97-H/negative	5	21.83 ± 0.21	20.72 ± 0.10	0.97 ± 0.04	2.922*	0.073
MHCC97-H/shRNA	5	24.24 ± 0.55	20.80 ± 0.14	0.20 ± 0.05	71.793*	< 0.001

\*Compared with the MHCC97-H/mock group. n, number of independent sample

**Table 3.** Effects of ANXA2 silencing on MHCC97-H cell cycles

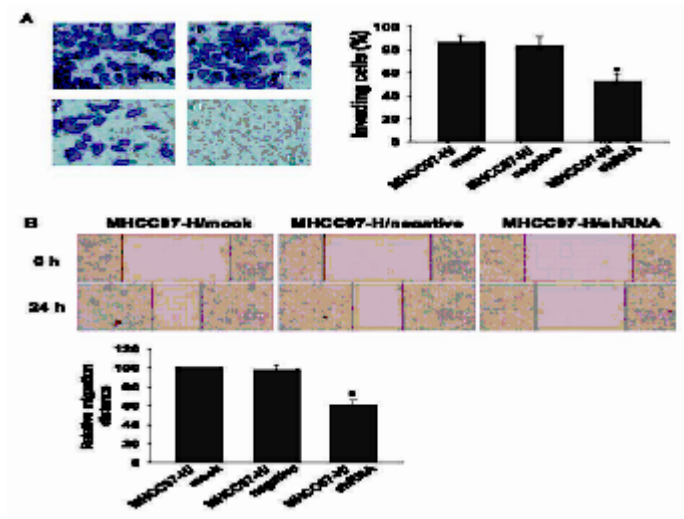
Group	n	G <sub>0</sub> -G <sub>1</sub> phase	G <sub>2</sub> -M phase	S phase
MHCC97-H/mock	5	50.05 ± 0.17	13.82 ± 1.23	36.14 ± 2.10
MHCC97-H/negative	5	49.10 ± 0.28*	14.68 ± 0.86	36.23 ± 1.07
MHCC97-H/shRNA	5	55.37 ± 0.68*	16.87 ± 1.12 <sup>y</sup>	27.76 ± 1.53 <sup>z</sup>

\*P<0.05 vs. the G<sub>0</sub>-G<sub>1</sub> phase of the MHCC97-H/mock group; <sup>y</sup>P<0.05 vs. the G<sub>2</sub>-M phase of the MHCC97-H/mock group; and <sup>z</sup>P<0.05 vs. the S phase of the MHCC97-H/mock group. n, number of independent sample.

of HCC cells. ANXA2 is a potential therapeutic target in angiogenesis and tumor metastasis (Zheng and Jaffee, 2012).

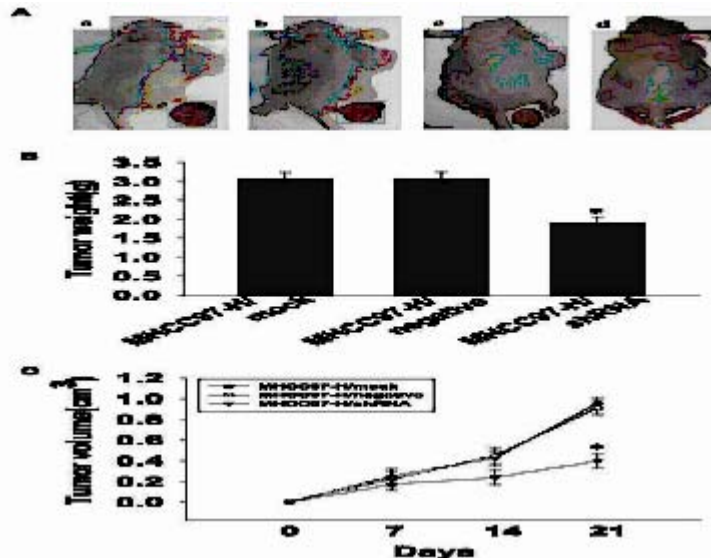
**ANXA2 down-regulation inhibited xenograft tumor growth**

Effect of ANXA2 down-regulation on tumor growth in vivo is shown in Figure 5. ANXA2



(A) Representative photos of the cells passing through the 8-µm pore stained with crystal violet at the right (400 × mag.). a, the MHCC97-H/mock group; b, the MHCC97-H/negative group; c, the MHCC97-H/shRNA group; and d, the blank control group (N=3, mean ± SD). (B) Representative photos of cell migration at various time points on the upper part (100 × mag.).

**Fig. 4.** ANXA2 lack down-regulated the invasion and migration potential of MHCC97-H cells



(A) Tumor-bearing nude mice appeared obvious emaciation, especially the former two. (B) Tumor weight showed a significant decrease comparing with that of MHCC97-H/mock group (\* $P < 0.05$ ), and inhibiting rate of tumor was 38.24%. (C) Each point represented the mean of tumor volume of each group at different time, and the results were given as mean ± SD.

**Fig. 5.** ANXA2 silencing inhibited xenograft tumor growth in vivo.

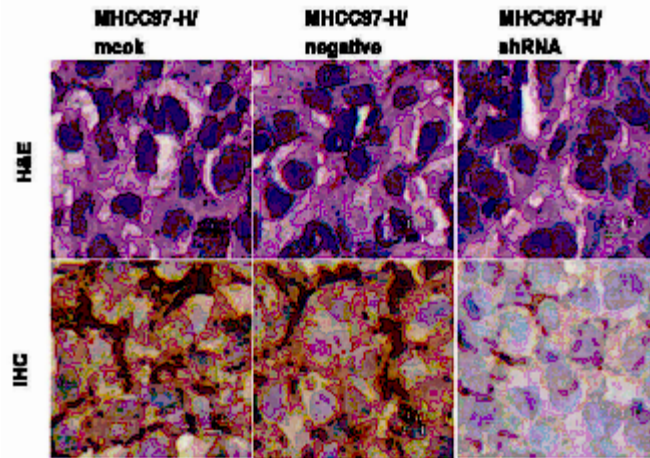


Fig. 6. ANXA2 expression in subcutaneous xenograft tumor

facilitated the cell cycle in cancer cell proliferation partly through the regulation of p53 via JNK/c-Jun (Wang CY., et al., 2012). ANXA2 silencing inhibited HCC progression or increased ANXA2 promoted cell proliferation following HCC development.

**ANXA2 expression and morphological alteration of xenograft tumor**

ANXA2 expression and characteristics of subcutaneous tumor xenografts are shown in

Figure 6 and Table 4. Prospective studies could facilitate patient stratification and therapeutic decisions at early stage, therefore affecting the clinical outcome (Behne and Copur, 2012). Specific shRNA suppressed obviously the proliferation of hepatoma cells with high metastasis potential and invasion possibly by promoting cell apoptosis mechanism.

Table 4. Intensity of ANXA2 expression in subcutaneous tumors of nude mice.

Group	n	N	ANXA2 intensity			Z	P
			+	++	+++		
MHCC97-H/mock	4	0	0	0	4		
MHCC97-H/negative	4	0	0	1	3	1.000*	0.317
MHCC97-H/shRNA	4	1	3	0	0	2.530*	0.011

\*Compared with the MHCC97-H/mock group. n, number of independent sample.

**ACKNOWLEDGEMENT**

This work was supported by grants-in-aid from Project of Health (BL2012053) of Jiangsu, the Int. Sci.&Tech. Cooperation Program (S2012ZR0031) and the Project (NO:81200634) of National Natural Science Foundation of China,

**REFERENCES**

1. Behne T, Copur MS., Biomarkers for hepatocellular carcinoma. *Int. J. Hepatol.*, 2012;

859076.  
 2. DuBray BJ, Jr., Chapman WC, Anderson CD Hepato- cellular carcinoma: a review of the surgical approaches to management. *Mo. Med.*, 2011; **108**:195-198.  
 3. El-Serag HB., Hepatocellular carcinoma. *N. Engl. J. Med.*, 2011; **365**: 1118-1127.  
 4. Forner A, Llovet JM, Bruix J., Hepatocellular carcinoma. *Lancet.*, 2012; **379**:1245-1255.  
 5. Gao J, Zhu J, Li HY, Pan XY, Jiang R, Chen JX., Small interfering RNA targeting integrin-linked kinase inhibited the growth and induced apoptosis in human bladder cancer cells. *Int. J.*

- Biochem. Cell. Biol.*, 2011; **43**:1294-1304.
6. Ruan J, Liu F, Chen X, Zhao P, Su N, Xie G, Chen J, Zheng D, Luo R., Inhibition of glypican-3 expression via RNA interference influences the growth and invasive ability of the MHCC97-H human hepatocellular carcinoma cell line. *Int. J. Mol. Med.*, 2011; **28**: 497-503.
  7. Saxena V, Lai CK, Chao TC, Jeng KS, Lai MM., Annexin A2 is involved in the formation of hepatitis C virus replication complex on the lipid raft. *J. Virol.*, 2012; **86**:4139-4150.
  8. Sharma M, Ownbey RT, Sharma MC., Breast cancer cell surface annexin II induces cell migration and neoangiogenesis via tPA dependent plasmin generation. *Exp. Mol. Pathol.*, 2010; **88**:278-286.
  9. Wang D, Xu MR, Wang T, Li T, Zhu J., MTSS1 overexpression correlates with poor prognosis in colorectal cancer. *J. Gastrointest. Surg.*, 2011; **15**: 1205-1212.
  10. Wang YL, Zhu ZJ, Teng DH, Yao Z, Gao W, Shen ZY., Glypican-3 expression and its relationship with recurrence of HCC after liver transplantation. *World. J. Gastroenterol.*, 2012; **18**: 2408-2414.
  11. Zhang J, Guo B, Zhang Y, Cao J, Chen T., Silencing of the annexin II gene down-regulates the levels of S100A10, c-Myc, and plasmin and inhibits breast cancer cell proliferation and invasion. *Saudi. Med. J.*, 2010; **31**:374-381.
  12. Zheng L, Jaffee EM., Annexin A2 is a new antigenic target for pancreatic cancer immunotherapy. *Onco-immunology.*, 2012; **1**: 112-114.